Properties of d- and k-type roughness in a turbulent channel flow

S. Leonardi[a)]
Department of Mechanical Engineering, University of Puerto Rico, 00680 Mayaguez, Puerto Rico

P. Orlandi
Dipartimento di Meccanica e Aeronautica Università, La Sapienza Via Eudossiana 18, 00184, Roma, Italy

R. A. Antonia
Discipline of Mechanical Engineering, University of Newcastle, Newcastle, NSW 2308, Australia

(Received 19 January 2007; accepted 25 September 2007; published online 17 December 2007)

Roughness is classified by the so-called roughness function, which represents the downward shift of the velocity profile relative to a smooth wall. The dependence of the roughness function on the Reynolds number is discussed with the aim of clarifying the difference between d-type and k-type behaviors. This difference has been traditionally associated with the stability of the flow within the roughness elements. The present direct numerical simulation results indicate that the difference more correctly reflects the different contributions from the frictional drag and pressure drag to the total stress. © *2007 American Institute of Physics*. [DOI: 10.1063/1.2821908]

I. INTRODUCTION

The different types of roughness that are encountered in engineering and environmental flows make it worthwhile trying to establish a meaningful classification for the roughness. The commonly accepted classification is based on the roughness function, or shift of the mean velocity profile relative to a smooth wall. The roughness function depends on the density, height, and nature of the roughness. A distinction was made between "k-" and "d-" type behavior (historically, "d" stands for the pipe diameter). In the context of a rough surface made up of transverse square bars, the cavity width w has to be larger than the height k in order to achieve a k-type behavior. For a k-type surface, ΔU^+ is a function of the roughness height (Hama[1] and Perry, Schofield, and Joubert[2]),

$$\Delta U^+ = \kappa^{-1} \ln k^+ + B, \tag{1}$$

where B depends on the nature and density of the roughness. Streeter and Chu[3] investigated the flow in three pipes with a square-threaded internal roughness, while Ambrose[4] studied a pipe with drilled circular holes. Equation (1) is not followed for either of the previous papers. On the other hand, Bisceglia *et al.*[5] found that, for two-dimensional square bars, the roughness function follows Eq. (1) but with $\kappa=0.61$. For the same surface, Perry *et al.*[2] did not find any correlation between ΔU^+ and k^+ and proposed that for this type of roughness, referred to as d-type, ΔU^+ should be given by

$$\Delta U^+ = \kappa^{-1} \ln d^+ + A, \tag{2}$$

where A depends on the nature and density of the roughness. These authors suggested that for a k-type roughness, eddies with length scale of order k are shed into the flow above the crests of the elements. Further away from the crests, these eddies diffuse into the flow. On the other hand, for a d-type rough wall, the elements are closely spaced, stable vortices form within the grooves, and there is essentially no eddy shedding into the flow above the elements. This explanation is not entirely correct since Djenidi, Elavarasan, and Antonia[6] found that, for $w/k=1$, there is vortex shedding out of the cavities, and the numerical results of Leonardi *et al.*[7] confirmed this. The ejections are less intense than those which occur when w/k is in the range 3 to 9 (i.e., for a k-type roughness), but the transition from $w/k=1$ to 3 and 9 appears to be rather gradual. Therefore, the abrupt transition between d-type and k-type behavior cannot simply reflect the state of the vortex shedding out of the cavities. Orlandi, Leonardi, and Antonia[8] introduced a new parametrization avoiding the use of an error in origin which can be a source of ambiguity. They found that the roughness function for both d- and k-type roughness, collapsed into a single curve when plotted against the rms wall-normal velocity at the crests plane. Since the rms velocity is correlated with the shedding out of the cavities, the nature and intensity of the shedding cannot explain the abrupt transition between d- and k-type roughness.

To our knowledge, Eq. (2) has yet to be validated convincingly, and the distinction between the two types of roughness remains unclear. For example, Tani *et al.*[9] suggested that a demarcation between k-type and d-type roughness might be made when the pitch to height ratio is equal to $w/k=3$. This surface has been identified by other authors as a k-type roughness (Perry *et al.*[2]). These disagreements are caused by difficulties in performing accurate measurements near the wall, in particular the measurements of U_τ and of the error in origin. The value of U_τ is often determined by the Clauser chart method. For smooth walls, George and Castillo[10] showed discrepancies between mean velocity profiles scaled using direct measurements of U_τ and approximations based on the Clauser chart. Wei, Schmidt, and McMurtry[11] showed that the Clauser chart method can mask a possible Reynolds number dependency near a wall. When the wall is rough, both the wall shear stress and the origin in

a)Author to whom correspondence should be addressed. Electronic mail: sleonardi@me.uprm.edu.

y are unknown. Perry *et al.*[12] outlined that several combinations of U_τ and error in origin are equally plausible for the same set of data, thus inducing uncertainties in the magnitude of the roughness function. Another way for estimating the wall shear stress is to neglect the frictional drag (see Perry *et al.*[2]). For square cavities, Bisceglia *et al.*[5] claimed to have a 10% error in the value of U_τ when they neglected the friction. Another source of error is caused by the machining of the rough surface. Perry *et al.*[2] showed that the results are particularly sensitive to the misalignment of the crests, especially for a d-type roughness.

Direct numerical simulations (DNSs), albeit at lower Reynolds numbers, provide reliable values of U_τ and error in origin. In the present paper, a new interpretation of d-type and k-type behavior is attempted by discussing DNS results for $w/k=1,1.5,3,7,9,59$ at three different Reynolds numbers: $\mathrm{Re}=2800,7000,12\,000$ ($\mathrm{Re}=U_b h/\nu$, $U_b=1/2h\int_{-h}^{h}Udy$ is the bulk velocity, h the channel half-width, and ν the kinematic viscosity, $k/h=0.1$). For a smooth wall channel, the corresponding values of Re_τ are 180, 380, and 600, respectively ($\mathrm{Re}_\tau=U_\tau h/\nu$ and U_τ is the friction velocity). Further simulations for $w/k=0.5$ and 1 ($0.15\leqslant k/h\leqslant 0.2$ and $\mathrm{Re}=2800,5000$) have been carried out in order to provide a larger number of cases with a d-type behavior. Triangular elements with $w/k=1$ have been considered to show the importance of the roughness shape in determining a d- or k-type behavior.

II. NUMERICAL PROCEDURE

The nondimensional Navier–Stokes and continuity equations for incompressible flows are

$$\frac{\partial U_i}{\partial t}+\frac{\partial U_i U_j}{\partial x_j}=-\frac{\partial P}{\partial x_i}+\frac{1}{\mathrm{Re}}\frac{\partial^2 U_i}{\partial x_j^2}+\Pi,\qquad \nabla\cdot U=0,\qquad (3)$$

where $\mathrm{Re}=(U_c h/\nu)$ is the Reynolds number, U_c is the centerline velocity, ν is the kinematic viscosity, Π is the pressure gradient required to maintain a constant flow rate, U_i is the component of the velocity vector in the i direction, and P is the pressure. The Navier–Stokes equations have been discretized in an orthogonal coordinate system using the staggered central second-order finite-difference approximation. Here, only the main features are recalled since details of the numerical method can be found in Orlandi.[13] The discretized system is advanced in time using a fractional-step method with viscous terms treated implicitly and convective terms explicitly. The large sparse matrix resulting from the implicit terms is inverted by an approximate factorization technique. At each time step, the momentum equations are advanced with the pressure at the previous step, yielding an intermediate nonsolenoidal velocity field. A scalar quantity Φ projects the nonsolenoidal field onto a solenoidal one. A hybrid low-storage third-order Runge–Kutta scheme is used to advance the equations in time. The roughness is treated by the efficient immersed boundary technique described in detail by Orlandi and Leonardi.[14] This approach allows the solution of flows over complex geometries without the need of computationally intensive body-fitted grids. It consists of imposing $U_i=0$ on the body surface which does not necessarily coincide with the grid. To avoid that the geometry is described in a stepwise way, at the first grid point outside the body, the second derivatives in the Navier–Stokes equations are discretized using the distance between the velocities and the boundary of the body rather than using the mesh size.

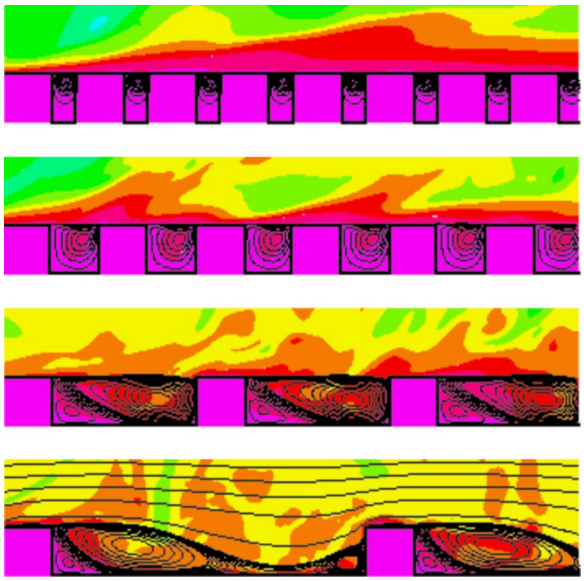

FIG. 1. (Color online) Instantaneous passive scalar contours superimposed on mean streamlines. From top to bottom, $w/k=0.5,1,3,7$.

III. MEAN FLOW

The main argument to support the difference between d-type and k-type roughness relies on the state of the vortex shedding (Perry *et al.*[2] and Ikeda and Durbin[15]). For the k-type roughness, eddies with length scale of order k are supposed to be shed into the flow above the crests of the elements. On the other hand, for a d-type rough wall, stable vortices form within the grooves and there is essentially no eddy shedding into the flow above the elements. Figure 1 shows passive scalar contours superimposed on mean streamlines for $w/k=0.5,1,3,7$. Contours for $w/k=0.5,1,3$ are rather similar even though the first two are usually classified as d-type while the latter is usually a k-type. On the other hand, despite differences in the passive scalar contours and mean streamlines (which reattach on the bottom wall), $w/k=7$ like $w/k=3$ is classified as k-type. It appears that a proper distinction between d-type and k-type roughness cannot be based on the state of the vortex shedding.

To clarify the difference between these two types of roughness, we discuss in detail how U_τ and ΔU^+ depend on the Reynolds number and on the nature of the roughness (in this case we consider different values of w/k and different roughness elements).

A. Friction velocity

On a rough wall, the total shear stress τ is the sum of the frictional drag ($\overline{C_f}$) and the pressure drag ($\overline{P_d}$). The frictional drag and pressure drag represent the integrals of the wall shear stress and pressure distributions, respectively, along the wall ($\overline{C_f}=\lambda^{-1}\int_0^\lambda\langle C_f\rangle\vec{s}\cdot\vec{x}ds$, $\overline{P_d}=\lambda^{-1}\int_0^\lambda\langle P\rangle\vec{n}\cdot\vec{x}ds$, s is a coordi-

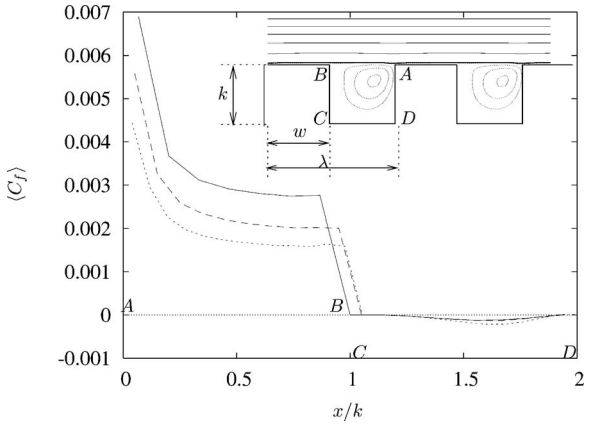

FIG. 2. Normalized (ρU_b^2) skin friction coefficient on the horizontal walls (the origin for x is at the leading edge) of a roughness element for $w/k=1$. Flow patterns for this geometry are shown in the inset: (—) Re=2800, (----) Re=7000, (·····) Re=12 000.

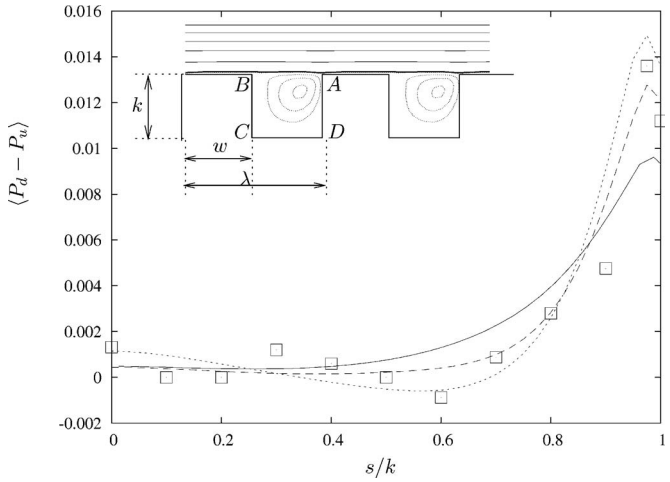

FIG. 3. Difference of pressure (normalized by ρU_b^2) along the vertical walls of the cavity for $w/k=1$ (P_d is on the side AD, P_u on BC): (—) Re=2800, (----) Re=7000, (·····) Re=12 000, (□) Perry (Ref. 2).

nate that follows the wall contour, $\vec{n}$ is a unit vector normal to the wall, $\vec{s}$ is a unit vector parallel to the wall, and $\vec{x}$ is the unit vector along x, angular brackets denote averaging with respect to z and t). Leonardi *et al.*[16] showed how the wall shear stress and pressure depend on w/k. We briefly recall here that, for $w/k<7$, the mean flow separates at the trailing edge of the element and reattaches on the upstream vertical wall of the element. For $w/k>7$, the flow reattaches on the bottom wall. As the next element is approached, the streamlines are tilted upwards and a new separation region is formed (see also Fig. 1). For $w/k=9$, Leonardi *et al.*[17] showed that the reattachment on the bottom wall moves towards the trailing edge as Re increases and the recirculation zone becomes smaller; on the roughness crests plane, the recirculation region (identified by the region where $\langle C_f \rangle$ is negative) is larger and more intense at larger Re. This is further corroborated here for $w/k=1$ by reference to the Reynolds number dependence in Fig. 2. The skin friction coefficient has a peak at the leading edge ($x=0$). It decreases on the roughness crests plane as Re increases. Within the cavity, the recirculating flow is quite weak and no appreciable effect can be observed. The dependence of pressure on the Reynolds number is weaker than that for the frictional drag. The distributions of pressure obtained by Leonardi *et al.*[17] for $w/k=9$ at three Reynolds numbers very nearly coincide. A larger dependence on the Reynolds number is observed for $w/k=1$. The difference in pressure along the vertical walls of the cavity is shown in Fig. 3. It is close to zero over nearly the full height of the roughness element and has a peak near the crests plane. The results agree reasonably well with Perry *et al.*[2] The frictional drag and pressure (or form) drag are obtained by integrating $\langle C_f \rangle$ and $\langle P_d \rangle$ over one wavelength. They are shown in Fig. 4 for three Reynolds numbers. By increasing the Reynolds number, the form drag differs by about 5% between Re=2800 and Re=12 000, while the frictional drag decreases appreciably (for $w/k=1$, it changes by about 50% between Re=2800 and Re=12 000). For $w/k=9$, the viscous drag is negligible with respect to the form drag, and consequently the total drag and hence U_τ depends only weakly on Re. This applies also to a three-dimensional (3D) roughness (Xie and Castro[18]). The opposite is true for $w/k=1$, the viscous drag being the main contributor to the total drag. The total drag and U_τ decreases as Re increases. The difference between the frictional and pressure drag decreases as Re increases.

B. Roughness function

The effect of the roughness is to shift the mean velocity profile, with respect to that on a smooth wall, by an increment ΔU^+, referred to as the roughness function, i.e.,

$$\langle U \rangle^+ = \kappa^{-1} \ln y^+ + C - \Delta U^+, \tag{4}$$

where C and κ are constants and "+" denotes normalization by either U_τ [$\equiv(\tau/\rho)^{1/2}$, τ is the sum of the frictional drag and form drags] or ν/U_τ. In Fig. 5, mean velocity profiles in wall units are shown up to $y_{\max}$, the location of the maximum streamwise velocity; $y_{\max}$ does not coincide with the centerline but is shifted upwards since the channel is asymmetric (Leonardi, Orlandi, and Antonia[19]). In the same figure, results for the smooth wall channel are reported for Re=2800 and Re=7000. There is good agreement with Kim *et al.*[20]

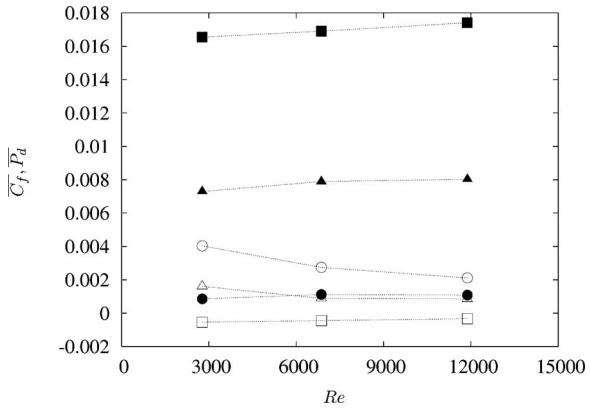

FIG. 4. Dependence of frictional and form drags (normalized by ρU_b^2) on the Reynolds number: (○) $w/k=1$, (△) $w/k=3$, (□) $w/k=9$. Empty symbols are for the frictional drag ($\overline{C_f}$), filled symbols are for pressure drag $\overline{P_d}$.

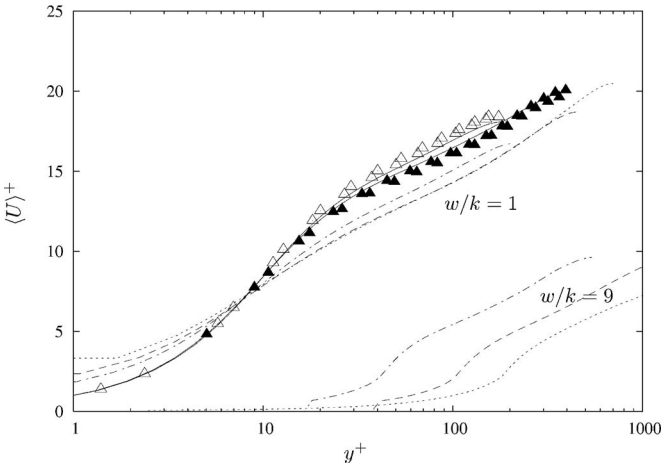

FIG. 5. Mean velocity in wall units: Solid lines, Kim *et al.* (Ref. 20), $\mathrm{Re}_\tau = 180$, and Moser *et al.* (Ref. 21), $\mathrm{Re}_\tau = 395$. Symbols represent simulations: (△) smooth wall channel, empty symbols Re=2800, filled symbols Re =7000. For the smooth wall channel, profiles on both walls are shown; for clarity, every fourth symbol is plotted. Broken lines are simulations for $w/k=1$ and $w/k=9$: (–––) Re=2800, (----) Re=7000, (·····) Re=12 000.

and Moser *et al.*[21] For $w/k=9$, although U_τ and ϵ/k do not vary with Re, the downward shift of $\langle U \rangle^+$ for Re=12 000 is larger than that for Re=7000 and 2800 (Fig. 5). This is due to the sideways shift produced by the different Re. In fact, $y^+ = y^* U_\tau^* / \nu^* = y h^* U_\tau U^* / \nu^* = y U_\tau \mathrm{Re}$, where a star indicates dimensional units. For $w/k=1$, the velocity distributions for Re=7000 and Re=12 000 overlap, while that for Re=2800 is only slightly different.

In Fig. 6, the values of the roughness function are plotted against k^+ for $w/k=1,3,9,59$. The values of k^+ are large enough for the flow to be considered fully rough (Bandyopadhyay[22]). For $w/k=3,9,59$, there is good agreement between the DNS data and Eq. (1) [recall that the value of B in Eq. (1) depends on w/k; i.e., the roughness density]. On the other hand, for $w/k=1$, the magnitude of ΔU^+ does not depend on k^+ so that a d-type roughness classification is appropriate. To further verify the independence of ΔU^+ on

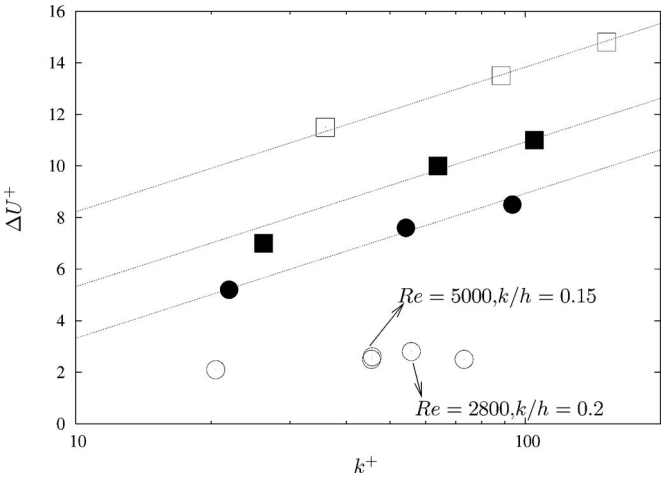

FIG. 6. Roughness function for $w/k=1,3,9,59$ for different values of k^+. Solid lines, Eq. (1) with $B=2.6, -0.3, -2.3$; (○) $w/k=1$; (■) $w/k=3$; (□) $w/k=9$; (●) $w/k=59$. Unless indicated, $k/h=0.1$.

k^+, two further simulations have been carried out with different values of Re and k/h. It is quite remarkable that two points relative to different simulations with different Re and k/h almost virtually coincide. We believe this is the first numerical evidence that square bars, with $w/k=1$, behave like a d-type roughness; i.e., ΔU^+ does not depend on k^+.

The different behaviors observed for d- and k-type roughness can be explained by examining how ΔU^+ depends on ϵ^+. Perry *et al.*[2] derived that, for both d-type and k-type surfaces,

$$\Delta U^+ = \kappa^{-1} \ln \epsilon^+ + B' . \tag{5}$$

Usually, the origin is inferred by fitting the mean velocity data to Eq. (4) after assuming $\kappa=0.41$. This origin lies between the crests plane and the bottom wall. An alternative strategy is to use the approach of Jackson[23] who identified ϵ with the centroid of the moment of forces acting on the elements. The two distributions agree quite well for small values of w/k, while larger differences are observed when w/k exceeds a value of about 5. The same discrepancy has been found by Coceal *et al.*[24] for 3D roughness. Although there are differences between the two values of the error in origin, Jackson's method is useful for providing some physical insight into the error in origin. For a k-type roughness, the contribution to the moment from $\overline{P_d}$ is large. The error in origin is proportional to k, viz., $\epsilon=\alpha k$, where α depends on the particular surface (here w/k) but does not depend on Re. Substituting $\epsilon=\alpha k$ into Eq. (5), Eq. (1) applies and its validity is verified in Fig. 6. For a d-type roughness, $\overline{P_d}$ is small, so that $\overline{C_f} k$ provides the main contribution to the moment and $\epsilon \sim 0$, implying that the origin is virtually on the crest. Hence, ϵ is approximately zero and represents a singularity of Eq. (5). Since the dependence with k is always associated with ϵ [through Eq. (5)] and in this case $\epsilon=0$, Eq. (1) does not apply. Therefore, ΔU^+ does not depend on k^+ (as verified in Fig. 6). The value $\epsilon=0$ reflects the fact that the frictional drag dominates over the pressure drag. The difference in the dependence of the roughness function on k^+, between d-type and k-type, does not rely on whether or not there is vortex shedding from the roughness elements. A d-type behavior ensues when the frictional drag dominates over the pressure drag, whereas for a k-type roughness the pressure drag is large. This claim is consistent with the abrupt transition between d-type and k-type behavior that has been observed in experiments. The d-type behavior is verified only for $\epsilon=0$, which is a singularity of Eq. (5). If the magnitude of the pressure drag is similar or larger than that of the frictional drag, $\epsilon=\alpha k$ and, as a consequence of Eq. (5), a k-type behavior applies.

To strengthen the above claim, two further sets of simulations were performed over rough walls with a slightly different geometry to that corresponding to the square cavities; viz., $w=k$. For $w=1.5k$, the form drag becomes comparable to the frictional drag ($\overline{C_f}=0.0013$, $\overline{P_d}=0.001$ for Re=2800, $\overline{C_f}=0.001$, $\overline{P_d}=0.000\,96$ for Re=7000). When scaled on wall units, the velocity profiles do not overlap (Fig. 7), as for the d-type case, but the roughness function depends on k^+, viz., $\Delta U^+ = (1/0.41) \ln k^+ - 5$.

To further highlight the importance of the pressure con-

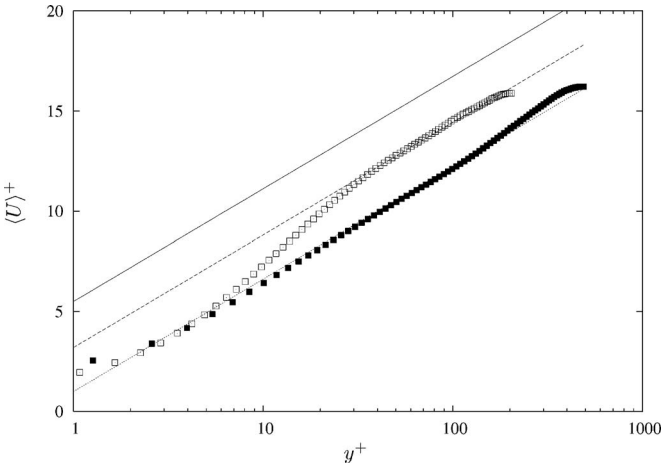

FIG. 7. Mean velocity in wall units. Lines: $U^+=(1/0.41)\ln y^+ + B$. (—) $B=5.5$; (----) $B=3.2$; (·····) $B=1$. Symbols: Square elements $w/k=1.5$; (□) Re=2800 and $k^+=20$; (■) Re=7000 and $k^+=50$.

tribution in determining whether the behavior is d- or k-type, the roughness elements have been modified slightly. Instead of square bars, triangular elements have been considered for the same pitch to height ratio (see inset in Fig. 8). The cavity, for $\lambda/k=2$ (note that, here, w is not constant, so it is more appropriate to use λ to denote the distance between the elements) is slightly larger than the square cavity. The angles at the base of the triangle are 63° instead of 90° for the square cavity. This small change in geometry results in a form drag which is significantly greater than the frictional drag ($\overline{C_f}=-0.0006$, $\overline{P_d}=0.0045$ for Re=2800, $\overline{C_f}=-0.0003$, $\overline{P_d}=0.0042$ for Re=7000). The friction is negative because the entire cavity is filled by a recirculating flow and the roughness crest, where the shear stress is positive and large, is reduced compared to the square bars. As a consequence of the increased form drag, the virtual origin is shifted downward with respect to the d-type case with $\epsilon=0.2k$. The mean velocity profiles, scaled on wall units, have a different roughness function given by $\Delta U^+=(1/0.41)\ln k^+ - 1$ (Fig. 8).

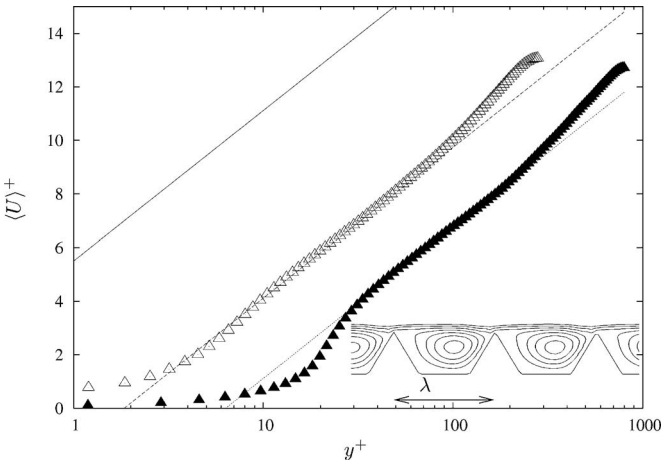

FIG. 8. Mean velocity in wall units. Lines: $U^+=(1/0.41)\ln y^+ + B$. (—) $B=5.5$; (----) $B=-1.5$; (·····) $B=-4.5$. Symbols: Triangular elements; (△) Re=2800 and $k^+=26$; (▲) Re=7000 and $k^+=75$.

While Eq. (1) is validated by the present results Eq. (2) [$\Delta U^+=\kappa^{-1}\ln d^+ + A$], is not verified (in the original paper d denotes the pipe diameter; there it corresponds to the channel width). In the present DNSs, the channel width is constant and then the values of d^+ are proportional to k^+. If, for a d-type the roughness function does not depend on k^+ (Fig. 6), it does not depend on d^+ either. For a rough channel, a d- or k-type behavior is in fact determined by the flow field near the rough wall (friction and pressure drag) and not by outer layer scales (d).

IV. CONCLUSIONS

The present paper is the first study which confirms that, for a so called d-type roughness, the roughness function does not depend on k^+. Present results agree with Eq. (1) (k-type behavior), but not with Eq. (2), which was proposed by Perry *et al.*[2] but is, as yet, unsupported by data. A new interpretation of the abrupt transition between d-type and k-type roughness is given in the present paper. The d-type behavior is obtained when the origin of y is on the crests plane and the frictional drag is much larger than the pressure drag. The important difference between d-type and k-type roughness is related to the relative magnitudes of the frictional and pressure drags.

ACKNOWLEDGMENTS

This research has been supported by MIUR 60% and the Australian Research Council. We thank Dr. Amati for his help with the code optimization, and the supercomputer center "Caspur" (www.caspur.it) for providing computing time.

[1] F. R. Hama, "Boundary layer characteristics over smooth and rough surfaces," Soc. Nav. Archit. Mar. Eng., Trans. **62**, 333 (1954).
[2] A. E. Perry, W. H. Schofield, and P. N. Joubert, "Rough wall turbulent boundary layers," J. Fluid Mech. **37**, 383 (1969).
[3] V. L. Streeter and H. Chu, Final Rep. Project 4918 Armour Res. Foundation, Illinois, 1949.
[4] H. H. Ambrose, Proc. ASCE, 1954, Vol. 80, SEP No. 491; Discussion of Proc. ASCE, 1954, Vol. 80, SEP No. 390.
[5] S. Bisceglia, R. J. Smalley, L. Djenidi, and R. A. Antonia, "Structure of rough wall turbulent boundary layers at relatively high Reynolds number," 14th Australasian Fluid Mechanics Conference, Adelaide University, Australia, edited by B. B. Daily, 2001, pp. 195–198.
[6] L. Djenidi, R. Elavarasan, and R. A. Antonia, "The turbulent boundary layer over transverse square cavities," J. Fluid Mech. **395**, 271 (1999).
[7] S. Leonardi, R. J. Orlandi, L. Djenidi, and R. A. Antonia, "Structure of turbulent channel flow with square bars on one wall," Int. J. Heat Fluid Flow **25**, 384 (2004).
[8] P. Orlandi, S. Leonardi, and R. A. Antonia, "Turbulent channel flow with either transverse or longitudinal roughness elements on one wall," J. Fluid Mech. **561**, 279 (2006).
[9] J. Tani, "Turbulent boundary layer development over rough surfaces," in *Perspectives in Turbulence Studies* (Springer, New York, 1987).
[10] W. K. George and L. Castillo, "Zero-pressure-gradient turbulent boundary layer," Appl. Mech. Rev. **50**, 689 (1997).
[11] T. Wei, R. Schmidt, and P. McMurtry, "Comment on the Clauser chart method for determining the friction velocity," Exp. Fluids **38**, 695 (2005).
[12] A. E. Perry and P. N. Joubert, "Rough wall boundary layers in adverse pressure gradients," J. Fluid Mech. **17**, 193 (1963).
[13] P. Orlandi, *Fluid Flow Phenomena: A Numerical Toolkit* (Kluwer Academic, Dordrecht, 2000).
[14] P. Orlandi and S. Leonardi, "DNS of turbulent channel flows with two- and three-dimensional roughness," J. Turbul. **7**, 1 (2006).
[15] T. Ikeda and P. A. Durbin, "Direct simulations of a rough-wall channel flow," J. Fluid Mech. **571**, 235 (2007).

[16]S. Leonardi, P. Orlandi, R. J. Smalley, L. Djenidi, and R. A. Antonia, "Direct numerical simulations of turbulent channel flow with transverse square bars on one wall," J. Fluid Mech. **491**, 229 (2003).
[17]S. Leonardi, F. Tessicini, P. Orlandi, and R. A. Antonia, "Direct numerical and large-eddy simulations of turbulent flows over rough surfaces," AIAA J. **44**, 2482 (2006).
[18]Z. Xie and I. P. Castro, "LES and RANS for turbulent flow over arrays of wall-mounted obstacles," Flow, Turbul. Combust. **76**, 291 (2006).
[19]S. Leonardi, P. Orlandi, and R. A. Antonia, "A method for determining the frictional velocity in a turbulent channel flow with roughness on the bottom wall," Exp. Fluids **33**, 31 (2005).
[20]J. Kim, P. Moin, and R. Moser, "Turbulence statistics in fully developed channel flow at low Reynolds number," J. Fluid Mech. **177**, 133 (1987).
[21]R. D. Moser, J. Kim, and N. N. Mansour, "Direct numerical simulation of turbulent channel flow up to $Re_\tau=590$," Phys. Fluids **11**, 943 (1999).
[22]P. R. Bandyopadhyay, "Rough-wall turbulent boundary layers in the transition regime," J. Fluid Mech. **180**, 231 (1987).
[23]P. S. Jackson, "On the displacement height in the logarithmic profile," J. Fluid Mech. **111**, 15 (1981).
[24]O. Coceal, T. G. Thomas, I. P. Castro, and S. E. Belcher, "Mean flow and turbulence statistics over groups of urban-like cubical obstacles," Boundary-Layer Meteorol. **121**, 491 (2006).